Mesenchymal stem cell-derived protein extract induces periodontal regeneration

Yihao Peng
Osaka Dental University: Osaka Shika Daigaku
Kengo Iwasaki
iwasaki-k@cc.osaka-dent.ac.jp
Osaka Dental University: Osaka Shika Daigaku https://orcid.org/0000-0002-0494-5760
Yoichiro Taguchi
Osaka Dental University: Osaka Shika Daigaku
Isao Ishikawa
Tokyo Medical and Dental University: Tokyo Ika Shika Daigaku
Makoto Umeda
Osaka Dental University: Osaka Shika Daigaku

Research Article

Keywords: Periodontal disease, regeneration, protein extracts, mesenchymal stem cells.

Posted Date: April 3rd, 2024

DOI: https://doi.org/10.21203/rs.3.rs-4156516/v1

Abstract

Background

Periodontal disease is characterized by chronic inflammation and destruction of supporting periodontal tissues, ultimately leading to tooth loss. In recent years, “cell-free treatment” without stem cell transplantation has attracted considerable attention for tissue regeneration. This study investigated the effects of extracts of mesenchymal stem cells (MSC-extract) and their protein components (MSC-protein) on the proliferation and migration of periodontal ligament (PDL) cells and whether MSC-protein can induce periodontal regeneration.

Methods

MSC-extract and MSC-protein were obtained by subjecting mesenchymal stem cells (MSCs) to freeze–thaw cycles and acetone precipitation. Cell proliferation was examined using a WST-8 assay and Ki67 immunostaining, and cell migration was examined using Boyden chambers. The MSC-protein content was analyzed using liquid chromatography-mass spectrometry, protein arrays, and enzyme-linked immunosorbent assays (ELISAs). Gene expression in MSC-protein-treated PDL cells was examined using RNA-sequencing and Gene Ontology analyses. The regenerative potential of MSC-protein was examined using micro-computer tomography (CT) and histological analyses after transplantation into a rat periodontal defect model.

Results

MSC-extract and MSC-protein promoted the proliferation and migration of PDL cells. Protein array and ELISA revealed that MSC-protein contained high concentrations of basic fibroblast growth factor (bFGF) and hepatocyte growth factor (HGF). Exogenous bFGF promoted the proliferation and migration of PDL cells. Furthermore, the transplantation of MSC-protein enhanced periodontal tissue regeneration with the formation of new alveolar bone and PDLs.

Conclusions

These results indicate that the MSC-protein promotes the proliferation and migration of PDL cells and induces significant periodontal tissue regeneration, suggesting that the MSC-protein could be used as a new cell-free treatment for periodontal disease.

Significance Statement

This study provides novel evidence that MSC protein extracts promote key phenomena of periodontal tissue regeneration, including PDL cell proliferation and migration, and induce periodontal tissue regeneration. As periodontal tissue regeneration restores the supporting tissues of teeth destroyed by periodontal disease and extends the life of teeth, MSC-protein transplantation, as discovered in this study,

may offer a new cell-free approach to regenerative therapies for periodontal disease that avoids the safety and cost concerns associated with conventional stem cell transplantation methods.

Introduction

Periodontal disease is a destructive disease of periodontal tissues caused by pathogenic factors derived mainly from gram-negative bacteria.[1, 2] The prevalence of periodontal disease is high and it is a major oral problem globally.[3] As periodontal disease progresses, chronic inflammation destroys the periodontal tissues that support the teeth (the gums, alveolar bone, periodontal ligament (PDL), and cementum), eventually leading to tooth extraction.[4] Various attempts have been made to regenerate periodontal tissues, and several regenerative therapies have been applied in clinical practice. However, the extent of tissue regeneration and the indications for these treatment methods are limited, and there is still a strong need for the development of new periodontal regenerative therapies. The PDL is a thin, soft tissue located between the tooth and bone that plays important roles in wound healing and homeostasis of periodontal tissues by supplying stem/progenitor cells to surrounding tissues and buffering occlusal forces on the tooth. The wound healing of periodontal tissue is dictated by the type of cells that migrate to and proliferate in the area of wound healing.[5, 6] It has been shown that periodontal tissue regeneration occurs only when PDL-derived cells migrate and proliferate to the site of wound healing, suggesting that proliferation/migration of the PDL is the key to regenerating new periodontal tissues.

Mesenchymal stem cells (MSCs) were originally isolated from bone marrow fluid as colony-forming plastic adherent fibroblastic cells.[7] They have been shown to differentiate into adipocytes, osteoblasts, and chondrocytes in vitro and ectopically form bone and cartilage in vivo, and are currently considered to be stem cells of mesenchymal tissues.[8] In addition to their differentiation potential, MSCs possess immunomodulatory, anti-apoptotic, angiogenic, and anti-inflammatory properties, and are currently being widely studied for use in regenerative therapies for various diseases.[9, 10] Although the regeneration mechanisms of MSCs are not fully understood, it has been shown that the humoral factors released by MSCs are responsible for a large part of the therapeutic effect of MSC transplantation.[11–13] Regenerative therapy by stem cell transplantation has disadvantages, such as potential tumorigenicity, cell source security, cell batch-dependent heterogeneity of its effect and treatment cost.[14–17] However, treatment using humoral factors avoids these problems and has recently gained attention as a “cell-free treatment”.[18, 19] MSC paracrine factors are generally recovered from culture supernatants; however, released humoral factors are diluted in the culture medium, resulting in low concentrations. Proteins, microvesicles, and other MSC paracrine factors are formed intracellularly and are temporarily stored in cells; therefore, these molecules can be recovered as cell extracts by disrupting the cell membrane.

We have previously reported that a cellular extract of MSCs (MSC-extract) promotes the proliferation of PDL cells.[20] Furthermore, we determined that heat treatment of the MSC-extract significantly diminished cell proliferative activity, suggesting the contribution of the protein component contained in the MSC-extract. We hypothesized that protein extracts recovered from bone marrow MSCs (MSC-protein) might

have the ability to regenerate periodontal tissues. This study aimed to investigate the periodontal tissue regenerative potential of MSC protein extracts by examining the effects of MSC-protein on PDL cells, which play an important role in periodontal regeneration, in a rat periodontal defect model.

Materials and methods

Cell culture

Human PDL fibroblasts and the bone marrow-derived MSC line UE7T-13 were obtained from Lonza (Basel, Switzerland) and the Riken BioResource Research Center (Tsukuba, Japan), respectively. The cells were cultured in α-minimum essential medium (α-MEM, Thermo Fisher Scientific, Waltham, MA, USA) supplemented with 15% fetal bovine serum (FBS, HyClone, Logan, UT, USA), GlutaMax and antibiotic-antimycotic solution (Thermo Fisher Scientific). The UE7T-13 line is an immortalized clone of bone marrow-derived MSCs generated by transduction with the papillomavirus type 16 protein E7 and human telomerase reverse transcriptase.[21] We selected this cell line because of its greater potential for differentiation into osteoblasts, adipocytes, and chondrocytes than two other clonal cell lines (UBE6T-7 and UE6E7T-12) in our pilot study. For adipocyte differentiation, hMSC adipogenic differentiation medium (Lonza) was used according to the manufacturer's instructions, and adipocytes were stained with Oil Red O solution (Sigma-Aldrich, St. Louis, MO, USA) after 4 weeks of differentiation. For osteoblast differentiation, UE7T-13 cells were cultured in α-MEM containing L-ascorbic acid 2-phosphate (50 μg/mL, Sigma-Aldrich), dexamethasone (10^{-8} M, Sigma-Aldrich), and β-glycerophosphate (10 mM, Sigma-Aldrich) for 3 weeks and von Kossa staining was performed to visualize the mineral deposits using a commercially available kit (Polysciences, Warrington, PA, USA). For chondrocyte differentiation, pellet culture of UE7T-13 cells was performed using chondrogenic induction medium (Lonza) containing TGF-β3 for 4 weeks. Frozen sections of UE7T-13 spheroids were prepared and stained with Alcian blue (Nacalai Tesque, Kyoto, Japan).

Flow cytometry

UE7T-13 cells were harvested by trypsinization, fixed in 4% paraformaldehyde (PFA) (Nacalai Tesque, Kyoto, Japan) for 15 min, and then blocked with 5× Blocking One solution (Nacalai Tesque) for 15 min on ice. Thereafter, the cells (2×10^5) were incubated with the following antibodies on ice for 30 min: PE-conjugated anti-human CD29, CD44, CD45, and CD105 (1:20; BioLegend, San Diego, CA, USA); PE-conjugated normal mouse IgG1k (1:20; BioLegend); PE-conjugated anti-human CD19 (1:10; BD Bioscience, Franklin Lakes, NJ, USA); FITC-conjugated anti-human CD73 (1:20; Invitrogen); FITC-conjugated anti-human CD34 (1:10; BD Bioscience); FITC-conjugated anti-human CD90 (1:25; Abcam, Cambridge, UK); FITC-conjugated normal mouse IgG1k (1:20; BioLegend); APC-conjugated human CD14 (1:20; BioLegend); and APC-conjugated normal mouse IgG2a (1:20; ExBio, Vestec, Czech Republic). After the cells were washed with phosphate-buffered saline (PBS) containing 2% FBS, flow cytometric analysis was performed using a FACS Verse flow cytometer (BD Bioscience). All flow cytometry data were analyzed using Flow Jo software (BD Bioscience).

MSC-extract and protein collection

A schematic diagram of the MSC-extract and MSC-protein isolation process is shown in Fig. 2A. Briefly, UE7T-13 cells were harvested using 0.05% trypsin-ethylenediaminetetraacetic acid (trypsin-EDTA; Thermo Fisher Scientific), washed with α-MEM, and then suspended in PBS at a density of 10^6 cells/100 μL of PBS. The cell suspension was alternately placed in a liquid nitrogen and water bath at 37°C to disrupt the cell membranes through three cycles of freezing and thawing. Next, the cells were centrifuged at 15000 rpm at 4°C for 30 min, after which the cell membranes and other debris were deposited at the bottom of the tube. Cellular extracts were then obtained by filtration through a 0.22-μm pore size filter (Kurabo, Osaka, Japan). For MSC-protein isolation, the MSC-extract samples were mixed with four volumes of cold acetone (Nacalai Tesque). After vigorous vortex mixing, the mixture was stored at -20°C for 1 h to precipitate the protein. Following centrifugation at 15000 rpm for 15 min, the supernatant was removed, and the protein pellet was dissolved in PBS or saline using an ultrasonic shaker. The protein concentrations of the samples were measured using a bicinchoninic acid (BCA) protein assay kit (Toyobo). The MSC-extract and protein were stored at -20°C until further use.

Electrophoresis of MSC-extract and protein

To examine the protein contents of MSC-extract and MSC-protein, 7.5 μg of total protein was mixed with an equal volume of sample buffer (ExApply, ATTO Corporation, Tokyo, Japan) plus dithiothreitol (DTT) and boiled for 5 min. Thereafter, the samples were subjected to 10% acrylamide gel electrophoresis, and the proteins were separated by sodium dodecyl sulfate–polyacrylamide gel electrophoresis. After electrophoresis, the acrylamide gels were stained with Coomassie Brilliant Blue (Nacalai Tesque), and gel images were obtained using a gel documentation system (ChemiDoc XRS Plus, Bio-Rad, Hercules, CA, USA).

WST-8 proliferation assay

PDL cells were seeded in 96-well plates (3000 cells/well) in α-MEM supplemented with different concentrations of MSC-extract, MSC-protein, recombinant human basic fibroblast growth factor (bFGF) (Pepro-Tech, Cranbury, NJ, USA), or recombinant human hepatocyte growth factor (HGF) (BioLegend, San Diego, CA, USA). After 3 days, the proliferation of PDL cells was examined using WST-8 assay reagent (Dojindo, Kumamoto, Japan) according to the manufacturer's protocol. The cell proliferation rate was expressed as the absorbance at 450 nm.

Ki67 immunostaining

Ki67 immunocytochemistry was used to examine proliferating cells. PDL cells were fixed with 4% PFA (Nacalai Tesque) for 20 min at room temperature, and the cells were permeabilized with 0.25% Triton X-100 in PBS for 15 min. Blocking of the cells was performed in 10% goat serum-PBS for 1 h. Primary antibody (mouse anti-human Ki67 antibody (DAKO, Tokyo, Japan)) and secondary antibody (goat anti-mouse IgG Alexa 488 (Thermo Fisher Scientific)) were applied to the PDL cells. After nuclear staining with Hoechst 33342 (Dojindo), the cells were observed under a fluorescence microscope (BZ-9000, Keyence,

Osaka, Japan). The percentage of Ki67-positive PDL cells was calculated from the total nuclear counts and the number of Ki67-positive cells in 15 randomly selected microscopic field images.

Cell migration assay using a Boyden chamber

PDL cell migration was examined using a Boyden chamber. Chambers (Kurabo) with 8 μm pore membranes were placed in 24 well plates. PDL cells (10^5 cells in α-MEM without serum) were added to the upper chamber, and α-MEM containing MSC-extract, MSC-protein, bFGF, or HGF was added to the lower well. After 8 h of incubation, the chambers were washed, and the membranes were fixed in 4% PFA. The migrated cells were stained with 0.05% crystal violet (Nacalai Tesque), and images of the migrated cells were captured using a BZ-9000 microscope (Keyence).

Growth factor array and enzyme-linked immunosorbent assay (ELISA)

To investigate the wide range of growth factors in MSC-extract and MSC-protein, a dot-blot-based antibody array kit (Hunan growth factor array C1) (Ray Biotech, Norcross, GA, USA) was used, following the manufacturer's protocol. A total of 500 μg of MSC-extract or MSC-protein sample was applied to the dot-blot membrane. After the membrane was exposed to the chemiluminescent solution, dots representing the concentration of each growth factor in the sample were photographed using a ChemiDoc XRS Plus (Bio-Rad). The intensity of each dot was measured using ImageJ software and calculated as a percentage of the intensity of the positive control. To assess the amounts of bFGF and HGF in the MSC-extract and MSC-protein, the Human Fibroblast Growth Factor Basic ELISA MAX Deluxe Set (BioLegend) and Human Hepatocyte Growth Factor Sandwich ELISA Kit (Proteintech, Rosemont, IL, USA) were used according to the protocols provided.

Liquid chromatography-mass spectrometry (LC-MS/MS)

The protein content of the MSC-extract was analyzed using LC-MS/MS at Kazusa Genome Technologies Inc. (Chiba, Japan). Proteins were isolated from the MSC-extract through acetone precipitation and reduced with 10 mM DTT at 50°C for 30 min. The reduced protein samples were digested using Lys-C and trypsin at 37°C overnight. After desalinization and extraction, the peptides were dissolved in 3% acetonitrile-0.1% formic acid. Nano LC-MS/MS analysis was performed using a linear acetonitrile gradient (3 to 65%) on an UltiMate 3000 RSLC nano LC system (Thermo Fisher Scientific) coupled to a Q Exactive HF-X mass spectrometer (Thermo Fisher Scientific) in ESI positive mode for 40 min. The obtained MS data were further analyzed for the identification and quantification of peptides and proteins using Scaffold DIA (Matrix Science, Tokyo, Japan). Peptides and proteins with a false discovery rate (FDR) less than 1% were identified and quantified.

RNA-sequencing (RNA-seq) and Gene Ontology (GO) analysis

Twenty-four hours after MSC-protein treatment, total RNA was extracted from PDL cells using NucleoSpin RNA (Macherey-Nagel, Düren, Germany). Following DNase treatment of the RNA samples, the RNA concentration and OD260/280 values were measured using a Nanodrop 1000 spectrophotometer (Thermo Fisher Scientific) and were 0.142 and 0.15 μg/μL and 2.12 and 2.09 for RNA from PDL cells and MSC-protein treated PDL cells, respectively. Thirty microliters of each RNA sample was sent to Veritas International (Madrid, Spain) for RNA-seq analysis. After poly(A) enrichment of the RNA samples, libraries were constructed using the NEBNext Ultra II RNA Library Prep Kit for Illumina (New England Biolabs, Ipswich, MA, USA) and sequenced using a NovaSeq 6000 system (Illumina Inc., San Diego, CA, USA). Quality testing of the sequencing data was performed using FastQC (version 0.11.8), and low-quality reads were depleted using Trim Galore (version 0.6.4). After filtering the sequencing data, each read was mapped to the reference genome, GTCh38, using STAR software (version 2.7.4a). FeatureCounts (version 1.6.4) was used to count the reads mapped to each gene symbol, and gene expression comparisons were performed on TMM-normalized count data using edgeR (version 3.22.3). Genes with fold changes greater than 3 and less than 0.3333333 were defined as upregulated and downregulated genes, respectively. GO analysis of the upregulated genes was performed using gprofiler2 (version 0.2.1). Fisher's exact probability test was performed for terms registered in GO (biological process [BP], molecular function [MF], and cellular component [CC]) and Reactome, and a statistical analysis was performed to determine which terms were related to genes with variable expression. The results of GO analysis are depicted as a Manhattan plot with terms on the horizontal axis and log p-values on the vertical axis.

Rat periodontal defect models and MSC-protein transplantation

The animal experiments in this study were approved by the Osaka Dental University Institutional Animal Care and Use Committee (approved #21-07004 and 22-02025) before the initiation of the experiments. All animal experiments were conducted in accordance with the approved guidelines of the Science Council of Japan for proper animal experiments and the ARRIVE guidelines (https://arriveguidelines.org/). The ARRIVE checklist is included in Additional File 6. All animal experiments were performed between March and April 2022 at the Osaka Dental University Animal Facility. The experimental animals were housed in a specific pathogen-free (SPF) environment with free access to food and water. The periodontal defect model was created according to the procedure described in a previous study, with certain modifications.[22] Twelve male Sprague-Dawley (SD) rats (8–10 weeks of age) (Shimizu Laboratory Supplies, Kyoto, Japan) were anesthetized through intraperitoneal injection of medetomidine (Zenoaq, Fukushima, Japan), midazolam (Astellas Pharma Inc.,Tokyo, Japan), and butorphanol (Meiji Seika Pharma Co., Ltd., Tokyo, Japan). The gingival flap on the mesial side of the maxillary first molar was elevated and periodontal defects were created with a dental bur using a stereoscopic microscope. Thereafter, a hydrogel scaffold (2×2×2 mm) (MedGel, Nitta Gelatin Inc., Osaka, Japan) with MSC-protein (780 μg/mL) (experimental group) or saline (control group) was transplanted, and the gingival flap was closed using a 7 – 0 silk suture (Johnson & Johnson, New Brunswick, NJ, USA). One periodontal tissue defect was created in each animal. The gingival incision was minimized to reduce invasiveness toward the animal, and careful attention was given to invasion of the surrounding tissues. Fifty microliters of MSC-protein

(approximately 400 μg/mL) or saline was injected into the gingival tissues around the maxillary first molar 5 days after surgery. The sample size was determined from similar periodontal tissue defect models conducted previously to minimize the number of rats used in the experiment.[23] When postoperative observation revealed symptoms of anguish or rapid weight loss (> 20% of body weight), the animal was excluded from the experiment. In such instances, humane endpoints were applied, and the experiment was terminated by euthanasia with an intraperitoneal overdose of barbiturate. These criteria were established prior to the experiment; however, no animals were excluded from the experiment. Six rats were assigned to the experimental and control groups, all of which were used in subsequent analyses (12 rats in total). The assignment of experimental groups was made by a blinded third individual to minimize bias in the experiments and analyses and K.I. was aware of the group allocation in this study.

Histological analysis

Four weeks after the transplantation surgery, the rats were sacrificed with an overdose of barbiturate (Kyoritsu Seiyaku, Tokyo, Japan), and tissue blocks of the maxillae were collected. Following fixation of the blocks in 4% PFA (Nacalai Tesque) for 2 d, decalcification was performed in 2× K-CX solution (FALMA, Tokyo, Japan) for 3 d at 4°C. Paraffin-embedded sections were prepared and stained with hematoxylin and eosin (H&E) for histological analysis. For picrosirius red staining, after deparaffinization, the sections were stained with 0.1% picrosirius red in saturated picric acid (Muto Pure Chemicals, Tokyo, Japan) for 10 min at 37°C. Images were captured using a BZ9000 microscope (Keyence). The primary outcome measure in this study was the extent of periodontal regeneration. For this purpose, the lengths between the cementoenamel junction (CEJ) and the bottom of the periodontal defect and between the bone crest and the bottom of the defect were measured. Using these two length measurements, the bone height ratio was calculated and compared.

Microcomputed tomography (micro-CT) analysis

Periodontal tissue healing was evaluated using micro-CT (Skyscan 1275, Burka, Antwerp, Belgium). Rat maxillary samples were scanned after PFA fixation (1 mm copper filter, 360° rotation, 0.2° rotation step, high-resolution mode, voltage 100 kV, and current 60 μA). The scanned images were reconstructed using InstaRecon software (Burka). To compare periodontal tissue regeneration, ImageJ software was used to measure the exposed root surface area perpendicular to the maxillary proximal root on the reconstructed images.

Images

For cells and histological sections, images were obtained using X20 Plan Fluor ELWD DM and X10 Plan Apo objective lenses (Nikon, Tokyo, Japan) in a BX-9000 system (Keyence). The fluorescent samples were observed using GFP-B and DAPI-B filters (Keyence). Images of the migration assay filters were captured using a digital camera (EOS40D, Canon, Tokyo, Japan). All images were first placed in PowerPoint for Windows (Microsoft Corporation, Redmond, WA, USA), cropped as needed, and positioned for the layout. Each figure was then exported as a TIFF file, and the resolution was changed to 350 dpi or higher using image analysis software (GIMP for Windows, https://www.gimp.org/) and saved as a TIFF

or PDF file. The resolution of the acquired micrographs is shown in the figure legends. Adjustments of each color channel, threshold manipulation, signal range expansion/contraction, alteration of high-signal intensity, and averaging were not performed. The original gel and membrane images are included in Supplementary Figs. 6 and 7 in Additional File 5.

Statistical analysis

The data are expressed as the mean ± standard deviation (SD). To confirm the reproducibility of the experiment, at least three independent similar experiments were conducted, and representative data from the confirmed reproducible data are shown in the figures. All the data are plotted on a bar graph to show their variability. For the comparison of two groups, the variance between the two groups was tested and Student's t test was used for comparisons between two groups. For comparison of more than three experimental groups, one-way analysis of variance (ANOVA) followed by Tukey's test was performed. All the statistical analyses were performed using GraphPad Prism 9.0.0 for Windows (San Diego, CA, USA). Differences with $p < 0.05$ were considered significant in this study.

Results

MSC characteristics of UE7T-13 cells

To determine the MSC characteristics of UE7T-13 cells, we examined the expression of cell surface MSC markers and the ability of the cells to differentiate into osteoblasts, adipocytes, and chondrocytes in vitro. Figure 1A shows the results of flow cytometry analysis of the relevant markers. UE7T-13 cells were positive for CD44 (hyaluronic acid receptor), CD105 (endoglin), CD73 (5'-nucleotidase), CD90 (Thy-1), and CD29 (integrin-β1) and negative for CD19 (B lymphocyte surface antigen B4), CD45 (protein tyrosine phosphatase receptor type C/leukocyte common antigen), CD14 (lipopolysaccharide receptor, monocyte/macrophage antigen), and CD34 (hematopoietic stem cell marker). When differentiation into adipocytes was induced in UE7T-13 cells, numerous cells containing Oil Red O-positive lipid droplets were observed, and large amounts of von Kossa stain-positive mineral deposits were observed under conditions of differentiation into osteoblasts (Fig. 1B). Pellet culture of UE7T-13 cells in chondrocyte differentiation induction medium resulted in the formation of cartilage-like masses that were positive for Alcian blue staining (Fig. 1B). These results are consistent with the minimal criteria proposed by the Mesenchymal and Tissue Stem Cell Committee of the International Society for Cellular Therapy[24] and indicate that UE7T-13 cells possess MSC properties.

Effect of MSC-extract on PDL cell proliferation

MSC-extract and MSC-protein were obtained from UE7T-13 cells using the method depicted in Fig. 2A. Considering the effect of MSC-extract on the proliferation of PDL cells, which are important for periodontal tissue regeneration, MSC-extract increased the proliferation of PDL cells and the percentage of Ki67-positive cells. (Fig. 2B and C). These effects were significantly suppressed by heat treatment of MSC-extract. Since the proliferative effect of the MSC-extract on the PDL was considered to be largely

dependent on its protein component, we next extracted the protein component (MSC-protein) of the MSC-extract and examined its effect on the proliferation of PDL cells. As shown in Fig. 2D, the MSC-protein enhanced the proliferation of PDL cells in a concentration-dependent manner. Additionally, the MSC-protein enhanced the ratio of Ki67-positive PDL cells, indicating the cell growth activity of the MSC-protein (Figure E).

Protein contents of the MSC-extract and MSC-protein

Next, the protein fractions in the MSC-extract and MSC-protein were examined using sodium dodecyl sulfate polyacrylamide gel electrophoresis (SDS-PAGE). SDS-PAGE images of both the MSC-extract and MSC-protein samples showed a large number of bands for proteins ranging in size from a few to several hundred kDa (Fig. 2F), confirming that both contain a wide variety of protein components. For further comprehensive analysis of the proteins in the MSC-extract, we used shotgun proteomic techniques. This analysis detected 4388 protein components in the MSC-extract (Additional File 1). The top 20 proteins detected in the MSC-extract are shown in Fig. 2G and are dominated by enzymes, cytoskeletal proteins, and matrix proteins, which are quantitatively required for cellular homeostasis.

MSC-extract and MSC-protein promote the migration of PDL cells

Migration is another important property of PDL-derived cells that, along with cell proliferation, is associated with periodontal regeneration[5,6]. The effect of MSC-extract and MSC-protein on the migration of PDL cells was examined using the Boyden chamber assay. We treated the MSC-extract for 30 min at 65°C to induce protein denaturation and examined the effect of the protein fraction contained in the MSC-extract on PDL cell migration along with MSC-extract and MSC-protein. MSC-extract, heat-treated MSC-extract, and MSC-protein were applied to the lower wells, and PDL cells were applied to the upper chambers, which had an 8-μm pore membrane at the bottom (Fig. 3A). As demonstrated in Figs. 3B and C, MSC-extract and MSC-protein enhanced the migration of PDL cells to the lower well, and this effect was reduced by heat treatment of the MSC-extract. These results indicate that the MSC-extract can promote the proliferation and migration of PDL cells through the MSC protein component.

RNA-seq analysis of PDL cells after MSC-protein treatment

To examine the effects of MSC-protein treatment on PDL cells, changes in gene expression in cells treated with MSC-protein were comprehensively examined by next-generation RNA-sequencing. Overall, 884 genes were upregulated and 514 genes were downregulated by MSC-protein treatment in PDL cells (Additional Files 2 and 3). Enrichment analysis using g:Profiler was performed to characterize the genes with variable expression in PDL cells. GO terms that increased significantly included “mitotic cell cycle process,” “cell division,” "nuclear division,” and “microtubule cytoskeleton organization involved in mitosis” (Fig. 4A). Furthermore, pathway analysis revealed a number of pathways closely related to cell division and proliferation, such as “nuclear division,” “mitotic nuclear division,” “DNA replication,” and “regulation of mitotic cell cycle phase transition,” as shown in Fig. 4B. The list of genes included in each term in the GO analysis is shown in Additional File 4. These results suggest that the cell cycle and mitotic activity are increased in MSC-protein-treated PDL cells.

Growth factors in MSC-extract and MSC-protein

These observations suggest that growth factors in MSC-extract/MSC-protein may be important functional components. Next, we examined growth factors in the MSC-extract and MSC-protein using dot blot-based growth factor protein array analysis. The growth factor array simultaneously detected 41 growth factors and growth factor receptors (Supplementary Fig. 1, Additional File 5). Figure 5A and B show the results of this analysis. Various dots were observed on the membrane to which the extract was applied. Notably, bFGF and HGF were strongly expressed (Fig. 5A). Similarly, high expression levels of bFGF and HGF were observed in MSC-protein (Fig. 5B). To confirm the results of the growth factor array, bFGF and HGF levels in the MSC-extract and MSC-protein were determined using ELISA. MSC-extract and MSC-protein contained bFGF (MSC-extract: 27.02 ± 17.4 ng/10^6 cells, MSC-protein: 7.93 ± 4.49 ng/10^6 cells) and HGF (MSC-extract: 0.68 ± 0.53 ng/10^6 cells, MSC-protein: 0.40 ± 0.20 ng/10^6 cells). To further investigate the involvement of bFGF and HGF in MSC-protein-induced PDL proliferation, we examined the effects of neutralizing antibodies against bFGF and HGF and gene knockdown of bFGF and HGF by siRNA on PDL proliferation and found that none of the neutralizing antibodies or siRNAs affected MSC-protein-induced PDL proliferation (Supplementary Figs. 2A to 2D in Additional File 5). We then examined PDL proliferation when MSC-extract/protein equivalent amounts of recombinant bFGF and HGF were added exogenously and observed that HGF had no effect, whereas bFGF significantly enhanced PDL proliferation (Fig. 5C). When the effects of various concentrations of bFGF and HGF on PDL proliferation were examined, bFGF enhanced PDL proliferation in a concentration-dependent manner, whereas HGF did not affect PDL proliferation (Supplementary Figs. 2E and 2F in Additional File 5). However, the effect of bFGF was far greater than the plateau observed at approximately 270 ng/mL in the MSC-extract/protein. These results suggest that the failure of bFGF neutralizing antibodies and siRNAs to affect PDL proliferation may be due to the high concentrations of bFGF in the MSC-protein. Furthermore, when PDL migration was examined using bFGF and HGF at concentrations equivalent to those of the MSC-extract/protein, bFGF significantly enhanced PDL migration, whereas HGF had no effect (Fig. 5D). These results indicate that bFGF plays a major role in enhancing MSC-protein-induced PDL cell proliferation and migration.

MSC-protein induced periodontal tissue regeneration

The observation that MSC-protein contain large amounts of bFGF and HGF and enhance the proliferation and migration of PDL cells indicates that MSC-protein may induce periodontal regeneration. Next, we examined the periodontal regenerative potential of MSC-protein using a surgical periodontal defect model in rats. Figures 6A–C and Supplementary Fig. 3 (Additional File 5) show the method of surgical periodontal defect creation and MSC-protein application. The alveolar bone, PDL, dentin, and cementum of the proximal root of the maxillary first molars of the rats were removed to create a fenestration-type periodontal defect. MSC-protein or saline was applied to the defects using a hydrogel as the carrier. Figure 6D and Supplementary Fig. 4 (Additional File 5) show the micro-CT images 4 weeks after hydrogel transplantation, and Fig. 6E shows the quantitative data of the exposed root area for the control and

MSC-protein groups. Compared with those in the control group, the defects in the MSC-protein treatment group resulted in a smaller exposed root area after 4 weeks (control, 12033 ± 1807 vs MSC-protein, 9682 ± 1386; *p* value, 0.03; effect size, 1.46; confidence interval [CI], 0.09–2.6). In this animal model, some degree of spontaneous healing occurred, and the exposed root area was reduced; however, the exposed area was smaller in defects implanted with MSC-protein.

Tissue sections were prepared and histological analysis was performed to examine the detailed conditions of the regenerated tissues. Figure 7 and Supplementary Fig. 5 (Additional File 5) show the histological images at low (A) and high (BC) magnification in the control and MSC-protein groups. The proximal surface of the maxillary first molar near the bottom of the defect in the control group showed mainly connective tissue consisting of fibers and cellular components, whereas new PDL tissue rich in collagen fibers and blood vessels was observed between the new bone and cementum in the MSC-protein group (Fig. 7B). Collagen fibers in the new PDL space were stained with picrosirius red, as shown in Fig. 7B. Further magnification of the root surface revealed fibers running parallel to the root surface in the control group, whereas multiple bundles of fibers running obliquely from the cementum surface were observed in the MSC-protein group, with prominent Sharpey's fiber-like structures (Fig. 7C). Figure 7D shows a schematic diagram of the measurement of the amount of regenerated tissue in the histological sections. The bone healing ratios in the control and MSC-protein groups were 24.99 ± 6.57% and 40.8 ± 14.35%, respectively, with significantly greater bone formation rates in defects treated with MSC-protein (*p* value, 0.0339; effect size, 1.42; CI, 0.06–2.56) (Fig. 7E). These results indicate that the application of MSC-protein to periodontal defects enhances periodontal regeneration.

Discussion

PDL cells are considered the key cell type for the regeneration of periodontal tissues. The healing of periodontal tissue is dictated by the type of cells that migrate and proliferate to the site of wound healing, and the proliferation and migration of PDL-derived cells are essential for periodontal tissue regeneration.[5, 6] Therefore, we investigated the effects of MSC-extract and MSC-protein on PDL cell proliferation and migration and showed that MSC-extract treatment increased the proliferation and migration of PDL cells mainly through their protein components. These results indicate the potential of MSC-protein for the regeneration of periodontal tissues. Furthermore, we demonstrated that MSC-protein application could induce periodontal regeneration in vivo. MSC-extract, as well as the MSC-protein, are composed of diverse components, as shown by SDS-PAGE and LC-MS/MS, and their biological effects are the sum of the effects of these various factors. Although we were unable to identify all the factors responsible for periodontal regeneration in this study, our growth factor array and ELISA results revealed that the MSC-extract and MSC-protein were rich in bFGF and HGF. In particular, bFGF significantly enhanced PDL proliferation and migration in experiments in which recombinant protein was added exogenously and may contribute to a large part of the function of the MSC-protein. bFGF is known to be a growth factor with diverse functions, such as cell proliferation, angiogenesis, and cell migration.[25] It has also been shown to induce periodontal tissue regeneration when transplanted into periodontal defects, and is used

clinically in periodontal regenerative therapy.[26, 27] HGF is another multifunctional growth factor with c-MET as a receptor, and is known to affect processes such as stem cell homing, angiogenesis, cell proliferation and migration, cancer invasion, and organ regeneration.[28, 29] Cao et al. reported that transplantation of dental pulp stem cells with forced HGF expression into periodontal defects in minipigs enhanced alveolar bone.[30] These findings are consistent with our experimental data and support the notion that MSC-protein enhances the proliferation and migration of PDL cells and periodontal regeneration.

We observed that MSC-extract enhanced the proliferation and migration of PDL cells through its protein component, MSC-protein. Several studies have reported the effects of MSC-extracts on tissue regeneration. Mishra et al. created skin defects on the backs of immunocompromised mice, administered MSC-lysate locally, and observed rapid wound closure.[31] MSC lysate promoted re-epithelialization of skin defects, and MSC lysate promoted wound healing. In addition, Tak et al. conducted a double-blind clinical study on patients with androgenetic alopecia (AGA) and showed that hair regrowth was induced when an extract derived from adipose tissue stem cells was applied to the scalps of AGA patients, indicating the tissue regenerative ability of the extract.[32] MSC-extract obtained by freeze-thawing is a mixture of various cell-derived components such as DNA, RNA, lipids, intracellular organelles, and cell-derived vesicles in addition to protein components. Cell-derived DNA, RNA, and some protein components, such as danger-associated molecular patterns (DAMPs), are known to induce inflammation and other tissue reactions, and MSC extract transplantation may cause inflammatory reactions.[33] To the best of our knowledge, this is the first report of periodontal tissue regeneration using proteins extracted from MSCs. In this study, since the effect of MSC-extract on PDL cell proliferation and migration was mainly due to its protein components and because the exogenous addition of MSC-protein significantly induced PDL cell migration and proliferation, we investigated the effect of MSC-protein on periodontal regeneration in vivo. Whether MSC-extract or MSC-protein are more suitable for periodontal tissue regeneration should be investigated in the future.

In this study, we investigated the ability of MSC-protein to induce tissue regeneration in a periodontal defect rat model. However, the model has several limitations. First, periodontal defects were surgically created, and the effects of the chronic inflammatory microenvironment may not exist in this model. Second, the animals used in this study were relatively young and their ages differed from those of most periodontal patients. These limitations may result in differences in wound healing between animal studies and periodontal patients. Therefore, future studies with conditions similar to those observed in patients with periodontitis are needed.

Many preclinical studies have shown that MSC transplantation can induce periodontal regeneration.[34–36] Several clinical trials have shown that the transplantation of MSCs regenerates periodontal tissues in human[37, 38] and that MSC transplantation is a powerful tool for periodontal regeneration. However, although MSC transplantation has these advantages, it has several drawbacks. These include the potential for tumor formation, limitations of suitable cell sources for transplantation, cell batch-

dependent heterogeneity of therapeutic effects, and the high cost of treatment.[17] Regenerative therapy with MSC-proteins does not require cells to be transplanted; therefore, no possibility of tumorigenicity exists. Additionally, UE7T-13 is an immortalized cell line that can be easily and inexpensively cultured as a cell source. Moreover, UE7T-13 cells are free of batch heterogeneity and are minimally susceptible to cellular senescence during cell culture. This approach has the advantage of utilizing qualitatively uniform and large amounts of MSC-protein. Therefore, the MSC protein-based periodontal regeneration demonstrated in this study can serve as a novel treatment method without abovementioned disadvantages of MSC transplantation for periodontal regeneration.

Conclusion

To the best of our knowledge, this is the first study to report the regenerative potential of MSC protein extracts. This study showed that MSC-protein promote the proliferation and migration of PDL cells, an important phenomenon associated with periodontal regeneration, and that MSC-protein contain large amounts of bFGF and HGF. Furthermore, we determined that the application of MSC-protein to periodontal defects induced periodontal regeneration. The regenerative properties of MSC-protein may promote and improve regeneration of a wide range tissues and wound healing beyond periodontal tissues. Additionally, MSC-proteins have the potential to be a promising regenerative therapeutic strategy because they do not have problems associated with MSC transplantation. However, further studies are needed to investigate the therapeutic and tissue regenerative effects of MSC-protein in various diseases and tissue defect models. In conclusion, our results indicate that MSC-protein transplantation may be a novel cell-free treatment for periodontal regeneration and represents a new therapeutic approach for tissue regeneration.

Abbreviations

AGA
androgenetic alopecia
bFGF
fibroblast growth factor-basic
BP
biological process
CC
cellular component
CEJ
cemento-enamel junction
DAMPs
danger-associated molecular patterns
DTT
dithiothreitol

FBS
fetal bovine serum
FDR
false discovery rate
GO
Gene Ontology
HGF
hepatocyte growth factor
MF
molecular function
Micro-CT
micro-computed tomography
MSCs
mesenchymal stem cells
MSC-extract
MSC-derived cell extracts
MSC-protein
MSC-derived protein components
PBS
phosphate buffered saline
PDL
periodontal ligament
PFA
paraformaldehyde
SD
standard deviation

Declarations

Ethics approval and consent to participate

The animal experiments in this study were approved by the Osaka Dental University Institutional Animal Care and Use Committee (approved #21-07004 and 22-02025) before the initiation of the experiments. (1) Project titles were both “Effects of stem cell extracts on the wound healing process in periodontal defect tissue model.” (2) Name of the institutional approval committee was Osaka Dental University Institutional Animal Care and Use Committee. (3) Approval numbers were 21-07004 and 22-02025. (4) Date of approval were 2021.11/2 and 2022.3/18.

Consent for publication

Not applicable

Availability of data and materials

The datasets of RNA-seq analysis are registration to DDBJ Sequence Read Archive database (https://ddbj.nig.ac.jp) and are openly available with accession numbers DRR385360-DRR385361 (https://ddbj.nig.ac.jp/resource/sra-run/DRR385360) (https://ddbj.nig.ac.jp/resource/sra-run/DRR385361). The remaining data supporting the findings of this study are available in this manuscript and the supplementary materials.

Competing interests

The authors declare that they have no competing interests.

Funding

This study was supported by JSPS KAKENHI Grant Number 21K09906 from the Japan Society for the Promotion of Science. The funding body played no role in the design of the study, collection, analysis, and interpretation of the data or the writing of the manuscript.

Authors' contributions

Y.P. contributed to the collection and assembly of the data, conducted the data analysis and interpretation, and participated in manuscript writing. K.I. contributed to the conception and design of the study, provided financial support, provided study materials, participated in the collection and assembly of the data, and conducted the data analysis and interpretation. Y.T. provided administrative support, contributed to the provision of study materials, and participated in manuscript writing. I.I. provided administrative support and contributed to manuscript writing and final approval of the manuscript. U.M. provided administrative support, contributed to the provision of study materials, and participated in manuscript writing. All the authors have read and approved the final manuscript.

Acknowledgements

We would like to thank all the members of our research group for their support.

References

1. Darveau RP. Periodontitis: a polymicrobial disruption of host homeostasis. Nat Rev Microbiol. 2010;8:481–90.
2. Pihlstrom BL, Michalowicz BS, Johnson NW. Periodontal diseases. Lancet. 2005;366:1809–20.
3. Petersen PE, Ogawa H. The global burden of periodontal disease: towards integration with chronic disease prevention and control. Periodontol 2000. 2012;60:15–39.
4. Page RC, Kornman KS. The pathogenesis of human periodontitis: an introduction. Periodontol 2000. 1997;14:9–11.

5. Polimeni G, Xiropaidis AV, Wikesjö UME. Biology and principles of periodontal wound healing/regeneration. Periodontol 2000. 2006;41:30–47.
6. Melcher AH. On the repair potential of periodontal tissues. J Periodontol. 1976;47:256–60.
7. Friedenstein AJ, Chailakhyan RK, Gerasimov UV. Bone marrow osteogenic stem cells: in vitro cultivation and transplantation in diffusion chambers. Cell Tissue Kinet. 1987;20:263–72.
8. Bianco P, Robey PG, Simmons PJ. Mesenchymal stem cells: revisiting history, concepts, and assays. Cell Stem Cell. 2008;2:313–9.
9. Pittenger MF, Discher DE, Péault BM, et al. Mesenchymal stem cell perspective: cell biology to clinical progress. NPJ Regen Med. 2019;4:22.
10. Merimi M, El-Majzoub R, Lagneaux L, et al. The Therapeutic Potential of Mesenchymal Stromal Cells for Regenerative Medicine: Current Knowledge and Future Understandings. Front Cell Dev Biol. 2021;9:661532.
11. Caplan AI, Correa D. The MSC: an injury drugstore. Cell Stem Cell. 2011;9:11–5.
12. Timmers L, Lim SK, Hoefer IE, et al. Human mesenchymal stem cell-conditioned medium improves cardiac function following myocardial infarction. Stem Cell Res. 2011;6:206–14.
13. van Poll D, Parekkadan B, Cho CH, et al. Mesenchymal stem cell-derived molecules directly modulate hepatocellular death and regeneration in vitro and in vivo. Hepatology. 2008;47:1634–43.
14. Lukomska B, Stanaszek L, Zuba-Surma E, et al. Challenges and Controversies in Human Mesenchymal Stem Cell Therapy. Stem Cells Int. 2019;2019:9628536.
15. Musiał-Wysocka A, Kot M, Majka M. The Pros and Cons of Mesenchymal Stem Cell-Based Therapies. Cell Transpl. 2019;28:801–12.
16. Levy O, Kuai R, Siren EMJ, et al. Shattering barriers toward clinically meaningful MSC therapies. Sci Adv. 2020;6:eaba6884.
17. Iwasaki K, Peng Y, Kanda R, et al. Stem Cell Transplantation and Cell-Free Treatment for Periodontal Regeneration. Int J Mol Sci. 2022;23:1011.
18. Sandonà M, Di Pietro L, Esposito F, et al. Mesenchymal Stromal Cells and Their Secretome: New Therapeutic Perspectives for Skeletal Muscle Regeneration. Front Bioeng Biotechnol. 2021;9:652970.
19. Ferreira JR, Teixeira GQ, Santos SG, et al. Mesenchymal Stromal Cell Secretome: Influencing Therapeutic Potential by Cellular Pre-conditioning. Front Immunol. 2018;9:2837.
20. Peng Y, Iwasaki K, Taguchi Y, et al. The extracts of mesenchymal stem cells induce the proliferation of periodontal ligament cells. J Osaka Dent Univ. 2023;57:119–24.
21. Mori T, Kiyono T, Imabayashi H, et al. Combination of hTERT and bmi-1, E6, or E7 induces prolongation of the life span of bone marrow stromal cells from an elderly donor without affecting their neurogenic potential. Mol Cell Biol. 2005;25:5183–95.
22. Chew JRJ, Chuah SJ, Teo KYW, et al. Mesenchymal stem cell exosomes enhance periodontal ligament cell functions and promote periodontal regeneration. Acta Biomater. 2019;89:252–64.

23. Nagata M, Iwasaki K, Akazawa K, et al. Conditioned Medium from Periodontal Ligament Stem Cells Enhances Periodontal Regeneration. Tissue Eng Part A. 2017;23:367–77.
24. Dominici M, Le Blanc K, Mueller I, et al. Minimal criteria for defining multipotent mesenchymal stromal cells. The International Society for Cellular Therapy position statement. Cytotherapy. 2006;8:315–7.
25. Yun Y-R, Won JE, Jeon E, et al. Fibroblast growth factors: biology, function, and application for tissue regeneration. J Tissue Eng. 2010;2010:218142.
26. Murakami S, Takayama S, Kitamura M, et al. Recombinant human basic fibroblast growth factor (bFGF) stimulates periodontal regeneration in class II furcation defects created in beagle dogs. J Periodontal Res. 2003;38:97–103.
27. Kitamura M, Akamatsu M, Kawanami M, et al. Randomized Placebo-Controlled and Controlled Non-Inferiority Phase III Trials Comparing Trafermin, a Recombinant Human Fibroblast Growth Factor 2, and Enamel Matrix Derivative in Periodontal Regeneration in Intrabony Defects. J Bone Min Res. 2016;31:806–14.
28. Zhao Y, Ye W, Wang Y-D, et al. HGF/c-Met: A Key Promoter in Liver Regeneration. Front Pharmacol. 2022;13:808855.
29. Shao Z, Pan H, Tu S, et al. HGF/c-Met Axis: The Advanced Development in Digestive System Cancer. Front Cell Dev Biol. 2020;8:801.
30. Cao Y, Liu Z, Xie Y, et al. Adenovirus-mediated transfer of hepatocyte growth factor gene to human dental pulp stem cells under good manufacturing practice improves their potential for periodontal regeneration in swine. Stem Cell Res Ther. 2015;6:249.
31. Mishra PJ, Mishra PJ, Banerjee D. Cell-free derivatives from mesenchymal stem cells are effective in wound therapy. World J Stem Cells. 2012;4:35–43.
32. Tak YJ, Lee SY, Cho AR, et al. A randomized, double-blind, vehicle-controlled clinical study of hair regeneration using adipose-derived stem cell constituent extract in androgenetic alopecia. Stem Cells Transl Med. 2020;9:839–49.
33. Gong T, Liu L, Jiang W, et al. DAMP-sensing receptors in sterile inflammation and inflammatory diseases. Nat Rev Immunol. 2020;20:95–112.
34. Li Q, Yang G, Li J, et al. Stem cell therapies for periodontal tissue regeneration: a network meta-analysis of preclinical studies. Stem Cell Res Ther. 2020;11:427.
35. Gaubys A, Papeckys V, Pranskunas M. Use of Autologous Stem Cells for the Regeneration of Periodontal Defects in Animal Studies: a Systematic Review and Meta-Analysis. J Oral Maxillofac Res. 2018;9:e3.
36. Yan X-Z, Yang F, Jansen JA, et al. Cell-Based Approaches in Periodontal Regeneration: A Systematic Review and Meta-Analysis of Periodontal Defect Models in Animal Experimental Work. Tissue Eng Part B Rev. 2015;21:411–26.
37. Dhote R, Charde P, Bhongade M, et al. Stem Cells Cultured on Beta Tricalcium Phosphate (β-TCP) in Combination with Recombinant Human Platelet-Derived Growth Factor - BB (rh-PDGF-BB) for the

Treatment of Human Infrabony Defects. J Stem Cells. 2015;10:243–54.

38. Ferrarotti F, Romano F, Gamba MN, et al. Human intrabony defect regeneration with micrografts containing dental pulp stem cells: A randomized controlled clinical trial. J Clin Periodontol. 2018;45:841–50.

Figures

Figure 1

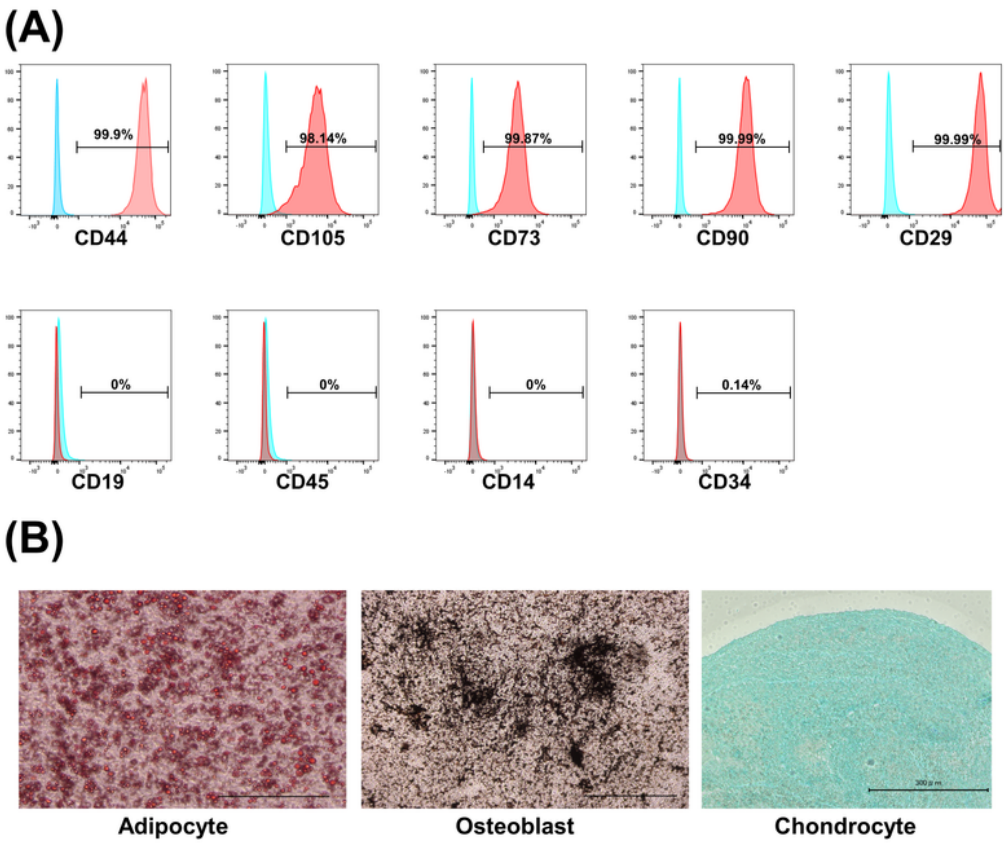

Figure 1

Characteristics of UE7T-13 cells as mesenchymal stem cells

(A) Cell surface marker expression profile of UE7T-13 cells. UE7T-13 cells were positive for MSC markers including CD44, CD105, CD73, CD90, and CD29 and negative for CD19 (B-cell marker), CD45 (leukocyte marker), CD14 (monocyte/macrophage marker) and CD34 (hematopoietic stem cell marker) in flow cytometry analysis. Red populations represent the experimental group, blue represents the respective isotype control, and the positivity rate for each marker is shown in each figure.

(B) Differentiation potential of UE7T-13 cells into adipocytes, osteoblasts, and chondrocytes. Oil red O staining (adipocyte, left), von Kossa staining (osteoblast, center), and Alcian blue staining (chondrocyte, right) were performed after the induction of UE7T-13 cell differentiation into adipocytes, osteoblasts, and chondrocytes. After adipocyte differentiation, many Oil Red O-positive (red) lipid droplets were observed at 4 weeks of induction of differentiation. After 21 days of differentiation, osteoblasts exhibited large amounts of von Kossa-stained mineral deposition (black). After 4 weeks of chondrocyte differentiation, the cartilage-like mass contained glucosaminoglycans which were stained with Alcian blue. Bar = 300 mm

Figure 2

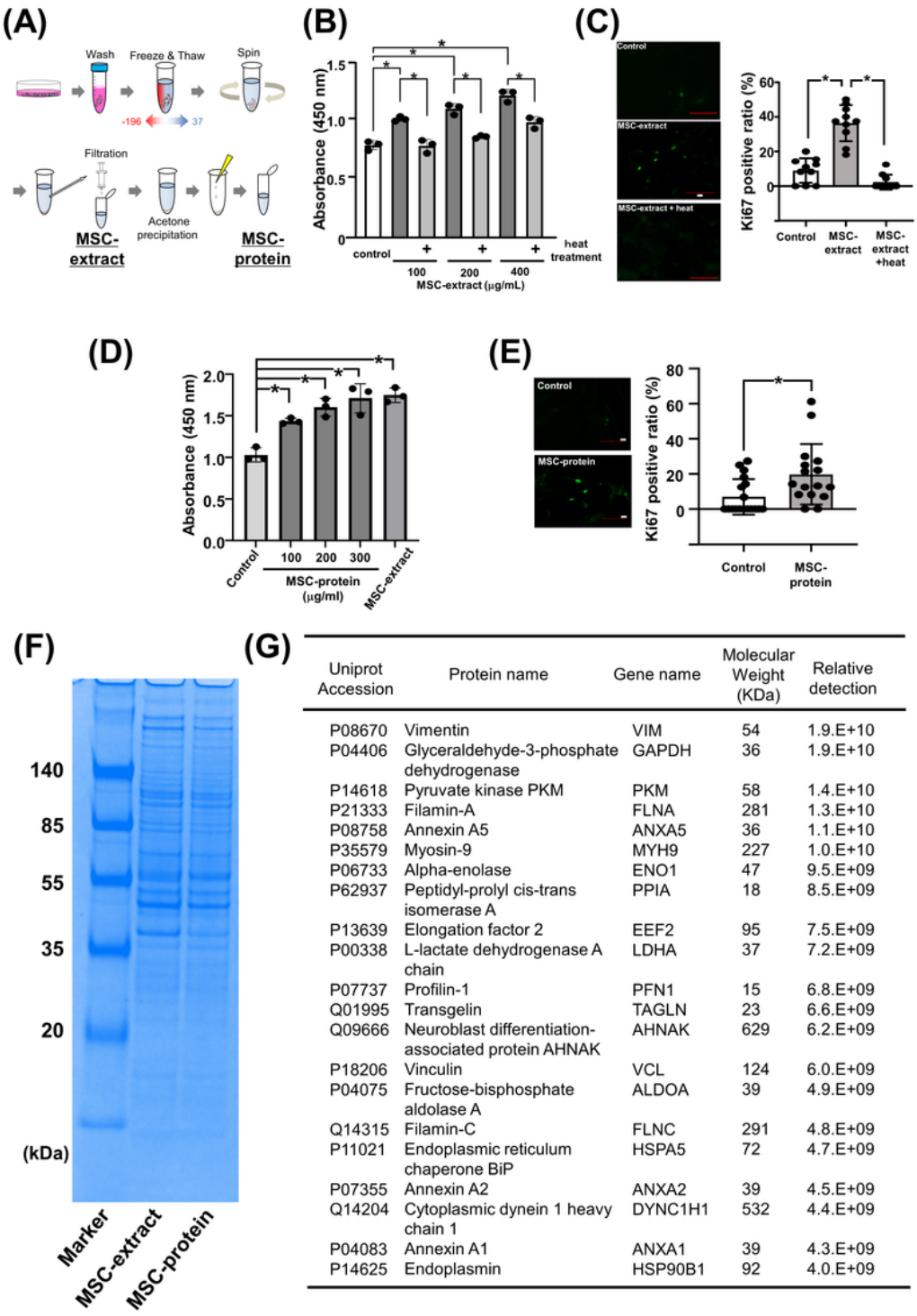

(G)

Uniprot Accession	Protein name	Gene name	Molecular Weight (KDa)	Relative detection
P08670	Vimentin	VIM	54	1.9.E+10
P04406	Glyceraldehyde-3-phosphate dehydrogenase	GAPDH	36	1.9.E+10
P14618	Pyruvate kinase PKM	PKM	58	1.4.E+10
P21333	Filamin-A	FLNA	281	1.3.E+10
P08758	Annexin A5	ANXA5	36	1.1.E+10
P35579	Myosin-9	MYH9	227	1.0.E+10
P06733	Alpha-enolase	ENO1	47	9.5.E+09
P62937	Peptidyl-prolyl cis-trans isomerase A	PPIA	18	8.5.E+09
P13639	Elongation factor 2	EEF2	95	7.5.E+09
P00338	L-lactate dehydrogenase A chain	LDHA	37	7.2.E+09
P07737	Profilin-1	PFN1	15	6.8.E+09
Q01995	Transgelin	TAGLN	23	6.6.E+09
Q09666	Neuroblast differentiation-associated protein AHNAK	AHNAK	629	6.2.E+09
P18206	Vinculin	VCL	124	6.0.E+09
P04075	Fructose-bisphosphate aldolase A	ALDOA	39	4.9.E+09
Q14315	Filamin-C	FLNC	291	4.8.E+09
P11021	Endoplasmic reticulum chaperone BiP	HSPA5	72	4.7.E+09
P07355	Annexin A2	ANXA2	39	4.5.E+09
Q14204	Cytoplasmic dynein 1 heavy chain 1	DYNC1H1	532	4.4.E+09
P04083	Annexin A1	ANXA1	39	4.3.E+09
P14625	Endoplasmin	HSP90B1	92	4.0.E+09

Figure 2

MSC-extract/protein enhanced PDL proliferation and contained various protein components

(A) Isolation of MSC-extract and MSC-protein from UE7T-13 cells. The cultured UE7T-13 cells were collected by trypsin treatment and washed, and the cell membrane was disrupted by three freeze-thaw cycles using liquid nitrogen and a water bath. The debris was then removed by centrifugation, and the

MSC-extract was filtered through a 0.22 mm pore size filter. Following acetone precipitation, the MSC-protein was dissolved in PBS or saline and stored.

(B) Enhancement of PDL cell proliferation by the MSC-extract and the effect of heating the MSC-extract on proliferation. The results of the WST-8 assay are shown after 72 hours of MSC-extract application to PDL cells. MSC-extract enhanced PDL cell proliferation dependent on its protein concentration. Heat treatment of MSC-extract diminished the enhanced proliferation of PDL cells induced by MSC-extract.

(C) Ki67 immunostaining in PDL cells. Fluorescence microscopy images of the control, MSC-extract and MSC-extract + heat groups are shown (left). The results of quantification of the Ki67-positive cell ratio are shown on the right. There were more Ki67-positive PDL cells in the MSC-extract group than in the control group, and heat of the MSC-extract reduced these cells. Bar=100 mm

(D) Enhancement of PDL cell proliferation by MSC-protein. The results of the WST-8 assay are shown after 72 hours of MSC-protein/extract application to PDL cells. MSC-protein increased PDL cell proliferation dependent on its protein concentration. MSC-extract served as a positive control.

(E) Ki67 immunostaining in PDL cells. Fluorescence microscopy images are shown for the control and MSC-protein groups (left). The quantification of Ki67-positive PDL cells is shown on the right. The percentage of Ki67-positive cells was determined from the number of Ki67-positeive cells and the nuclear count. The ratio of Ki67-positive PDL cells in the MSC-protein group was significantly greater than that in the control group.

(F) SDS-PAGE of the MSC-extract and MSC-protein. Images of SDS-PAGE gels of MSC-extract and MSC-protein are shown. Both the MSC-extract and MSC-protein showed many bands from low to high molecular weights.

(F) The top 20 protein components detected from MSC-protein by LC-MS/MS analysis. A list of the top 20 proteins with the highest number of hits in the LC-MS/MS analysis is shown. Enzymes and cytoskeletal proteins are frequently observed.

*$p < 0.05$; one-way ANOVA (Tukey test)

Figure 3

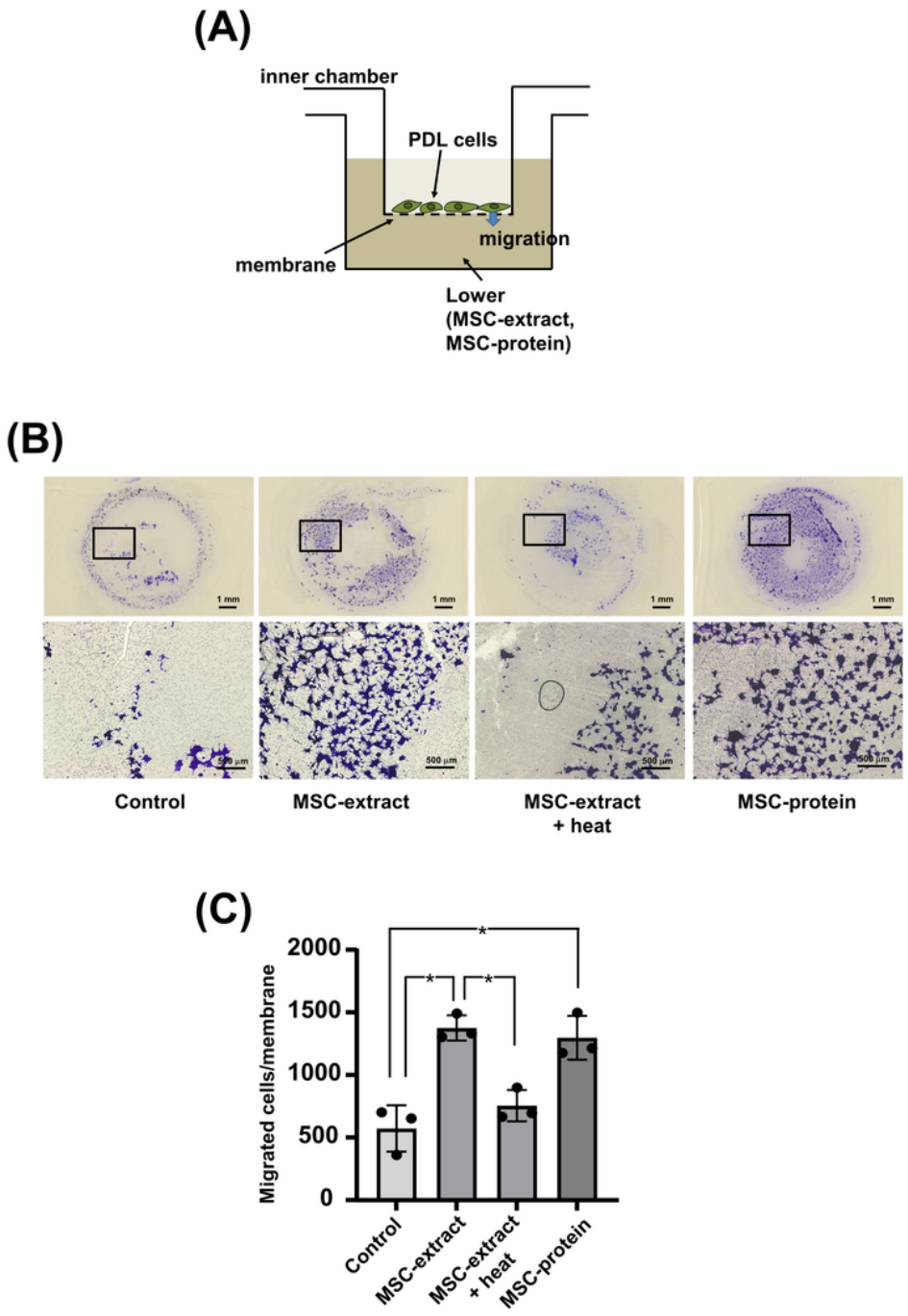

Figure 3

MSC-extract and MSC-protein promoted PDL cell migration

(A) Schematic diagram of the Boyden chamber assay. PDL cells in the chamber were separated from the MSC-extract/MSC-protein by a membrane with 8 mm pores. Cells that migrated to the underside of the membrane were examined.

(B) PDL cells migrating to the lower surface of the membrane. Crystal violet-stained images of the underside of the membrane are shown. Lower and higher magnified images are shown in the upper and lower panels, respectively. Many crystal violet-positive cells were found in the MSC-extract and MSC-protein groups, and fewer were found in the control and heat-treated groups. The original micrographs were taken at 72 dpi (upper panels) and 96 dpi (lower panels) and the resolution was enhanced using the methods described in the Materials and Methods. Bar = 1 mm (upper panels) or 500 mm (lower panels).

(C) Quantitative results of the Boyden chamber assay. The number of cells that migrated to the underside of the membrane was quantified. The number of migrated cells significantly increased in the MSC-extract and MSC-protein groups and decreased with heat treatment of MSC-extract. *$p < 0.05$; one-way ANOVA (Tukey test)

Figure 4

(A)

id	source	term_id	term_name	term_size	p_value
1	GO:BP	GO:1903047	mitotic cell cycle process	956	3.1e-36
2	GO:BP	GO:0007049	cell cycle	1867	1.1e-35
3	GO:BP	GO:0000278	mitotic cell cycle	1098	3.4e-35
4	GO:BP	GO:0022402	cell cycle process	1388	7.0e-35
5	REAC	REAC:R-HSA-1640170	Cell Cycle	679	7.0e-30
6	REAC	REAC:R-HSA-69278	Cell Cycle, Mitotic	549	4.9e-29
7	GO:BP	GO:0051301	cell division	630	5.5e-26
8	GO:BP	GO:0000280	nuclear division	495	1.4e-24
9	GO:BP	GO:1902850	microtubule cytoskeleton organization involved in mitosis	214	2.6e-24
10	GO:BP	GO:0007059	chromosome segregation	353	2.6e-24
11	GO:BP	GO:0048285	organelle fission	544	2.3e-23
12	GO:BP	GO:0007052	mitotic spindle organization	194	8.1e-23
13	GO:BP	GO:0000819	sister chromatid segregation	214	8.1e-22
14	GO:BP	GO:0098813	nuclear chromosome segregation	293	8.1e-22
15	GO:BP	GO:0140014	mitotic nuclear division	346	8.1e-22
16	REAC	REAC:R-HSA-69620	Cell Cycle Checkpoints	290	1.3e-21
17	GO:BP	GO:0007051	spindle organization	256	1.5e-21
18	GO:CC	GO:0098687	chromosomal region	348	1.5e-21
19	GO:BP	GO:0000070	mitotic sister chromatid segregation	185	4.0e-21
20	GO:BP	GO:0051726	regulation of cell cycle	1120	4.9e-20

g:Profiler (biit.cs.ut.ee/gprofiler)

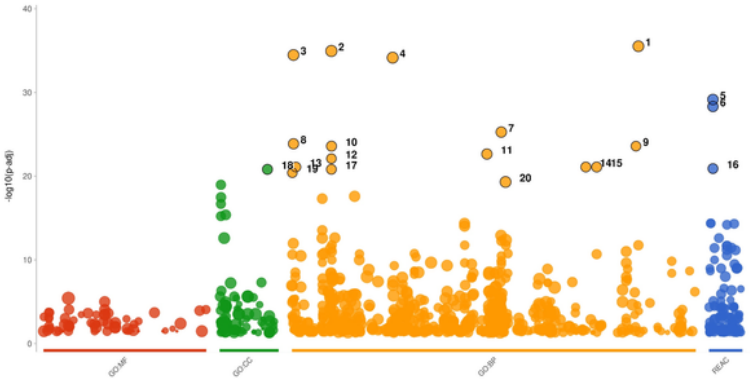

(B)

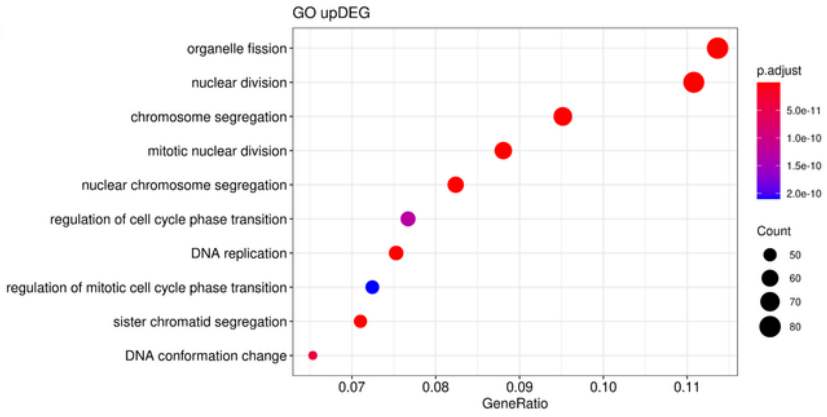

Figure 4

Results of GO analysis and pathway analysis of PDL cells after MSC-protein treatment

(A) Manhattan plot and the top 20 GO terms in the enrichment analysis using the RNA-seq data are shown. Many terms related to cell division and proliferation, such as "mitotic cell cycle process" and "cell

division," were frequently found. BP: biological process, MF: molecular function, CC: cellular component, REAC: Reactome

(B) Baloon plot created from the results of pathway analysis using the RNA-seq data is shown. Many of the enriched pathways were associated with cell proliferation and division.

Figure 5

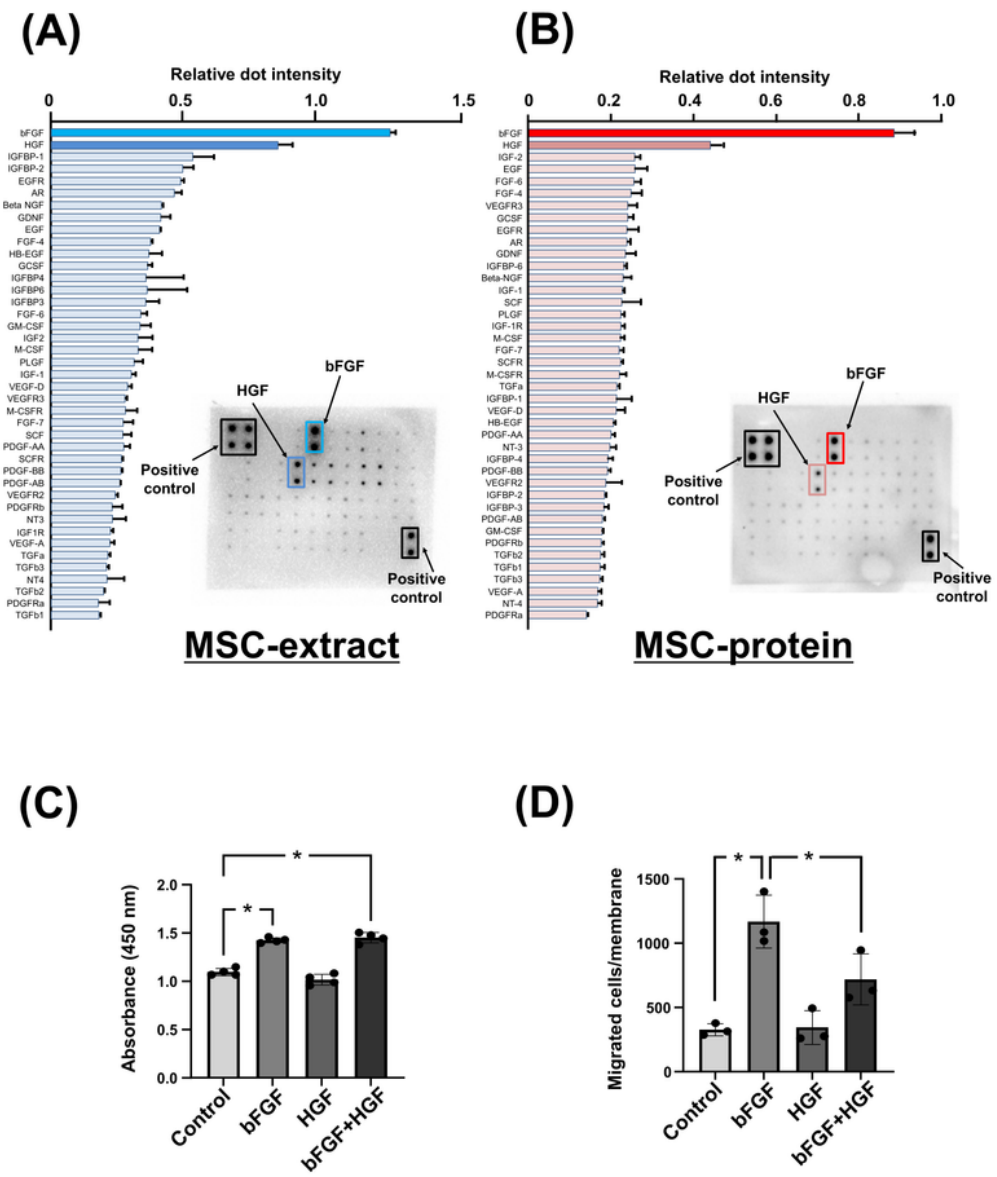

Figure 5

Growth factor array analysis of MSC-extract and MSC-protein, and the effect of exogenous bFGF and HGF on PDL cell proliferation and migration.

(A, B) Membrane images of growth factor arrays with MSC-extract (A) and MSC-protein (B) and the results of their quantification are shown. Both the MSC-extract and MSC-protein had the strongest expression of bFGF, followed by high expression of HGF.

(C) Effect of exogenous bFGF and HGF on PDL cell proliferation. Recombinant bFGF and HGF equivalent to MSC-extract (bFGF = 270 ng/mL, HGF = 7 ng/mL) were added to PDL cells and the results of the WST8 assay after 72 hours are shown. bFGF increased PDL cell proliferation while HGF had no effect on it. *$p < 0.05$; one-way ANOVA (Tukey test)

(D) Effect of bFGF and HGF on PDL cell migration. Recombinant bFGF and HGF equivalent to MSC-extract (bFGF = 270 ng/mL, HGF = 7 ng/mL) were applied to the lower chamber to examine PDL cell migration. Migrated PDL cell number/membrane was quantified and is shown. bFGF increased PDL cell proliferation, while HGF inhibited PDL cell proliferation when combined with bFGF. *$p < 0.05$; one-way ANOVA (Tukey test)

Figure 6

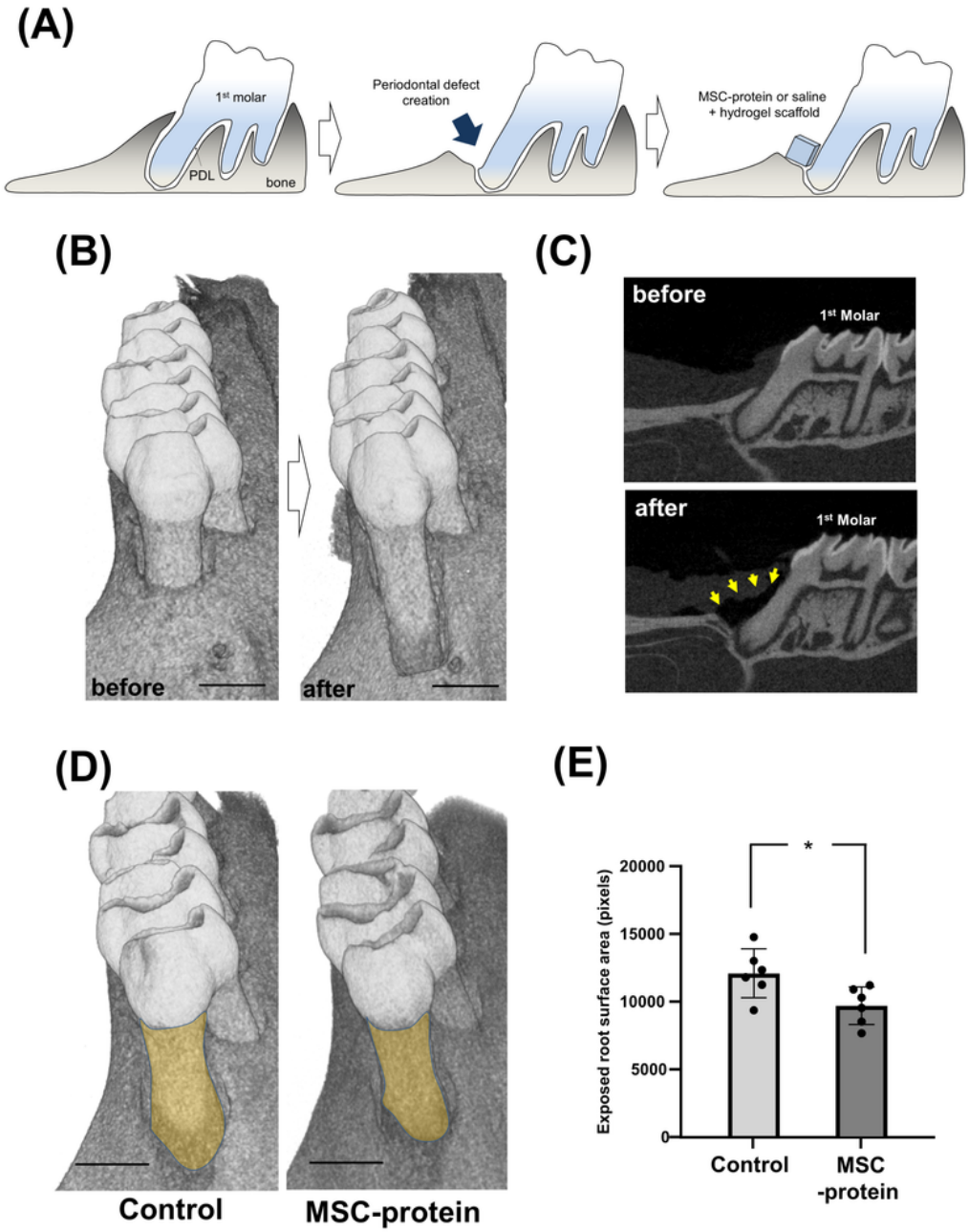

Figure 6

MSC-protein enhanced periodontal regeneration in a rat periodontal defect model

(A) Schema of periodontal defect creation and MSC-protein transplantation. The periodontal tissues on the proximal surface of the first molar were surgically removed to create a defect, and the MSC-protein was implanted using a hydrogel as a carrier. This schema was created by the authors.

(B) Micro-CT images before and after surgical defect creation. A defect 2.5 mm deep from the CEJ was created on the proximal surface of the first molar. The 3D constructed images are shown perpendicular to the first molar proximal root. Bar = 1 mm

C) Sagittal micro-CT images before and after defect creation. Periodontal defects were created by the removal of alveolar bone, periodontal ligament, cementum, and dentin. Yellow arrows: Periodontal defect

(D) Micro-CT images of the control and MSC-protein groups at 4 weeks after transplantation. 3D constructed images of the proximal root of the first molar in the control and MSC-protein groups are shown. The images are shown perpendicular to the proximal root. In the MSC-protein group, the exposed root surface area, shown in yellow, was reduced. Yellow: Exposed root surface area, Bar = 1 mm

(E) Exposed root surface area in the control and MSC-protein groups. The results of the quantification and comparison of the root surface area on 3D constructed micro-CT images from the control and MSC-protein groups are shown. In the MSC-protein group, the exposed root surface area was significantly smaller than that in the control group. *$p < 0.05$; Student's t test

Figure 7

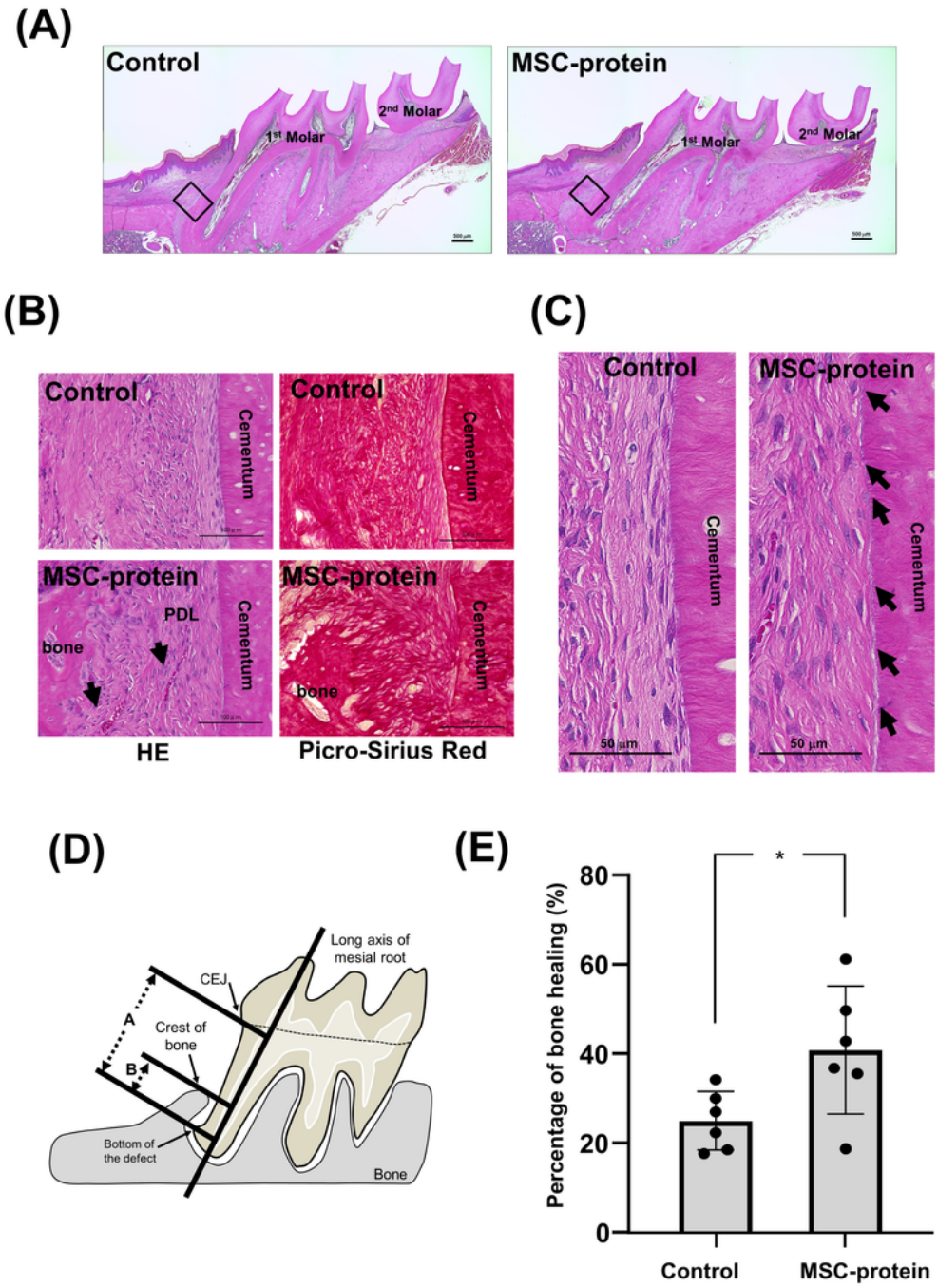

Figure 7

Histological analysis of regenerated periodontal tissues after MSC-protein transplantation

(A) Histology of the control and MSC-protein groups 4 weeks after transplantation. Lower magnified histological images of the control and MSC-protein groups are shown. The alveolar bone height around the proximal first molar was greater in the MSC-protein group than in the control group. The black boxes

are the fields of view shown in (B). The original micrographs were taken at 96 dpi and the resolution was enhanced using the methods described in Materials and Methods. Bar = 500 mm

(B) Histological images of the bottom of the bony defect. The higher magnified images in the frame shown in (a) are shown. The left panels show HE staining, and the right panels show picrosirius red staining of the control (upper) and MSC-protein (lower) groups. In the control group, connective tissue composed of fibers and cells was observed within the defect, while in the MSC-protein group, new alveolar bone and periodontal ligament with blood vessels were observed. The original micrographs were taken at 96 dpi, and the resolution was enhanced using the methods described in the Materials and Methods. Arrows: blood vessels in the PDL space; scale bar = 100 mm.

(C) Higher magnification images of the root surface. High-magnification images of the root surfaces in the control and MSC-protein groups are shown. In the control group, layers of fiber bundles running parallel to the cementum surface were observed. On the other hand, many bundles of fibers running obliquely from the cementum surface were observed in the MSC-protein group. The original micrographs were taken at 96 dpi, and the resolution was enhanced using the methods described in the Materials and Methods.Arrows: Fiber bundles from the cementum surface. Bar = 50 mm

(D) Quantification of bone formation on tissue specimens. The schema indicates measurements taken to compare the bone healing ratio in the tissue section. We measured the distance from the bottom of the defect to the CEJ (A) and the distance to the bone crest (B) based on the first molar proximal root tooth axis. This schema was created by the authors to illustrate the quantification method.

(E) Comparison of the percentage of healing by new bone formation. The percentage of healing by new bone in the control and MSC-protein groups was calculated and compared on histological images at 4 weeks. Bone healing rates were significantly greater in the MSC-protein group than in the control group. *$p < 0.05$; Student's t test

Supplementary Files

This is a list of supplementary files associated with this preprint. Click to download.

- Additionalfile1.Pengetal.xlsx
- Additionalfile2.Pengetal.xlsx
- Additionalfile3.Pengetal.xlsx
- Additionalfile4.Pengetal.xlsx
- Additionalfile5.Pengetal.pdf
- Additionalfile6.Pengetal.pdf